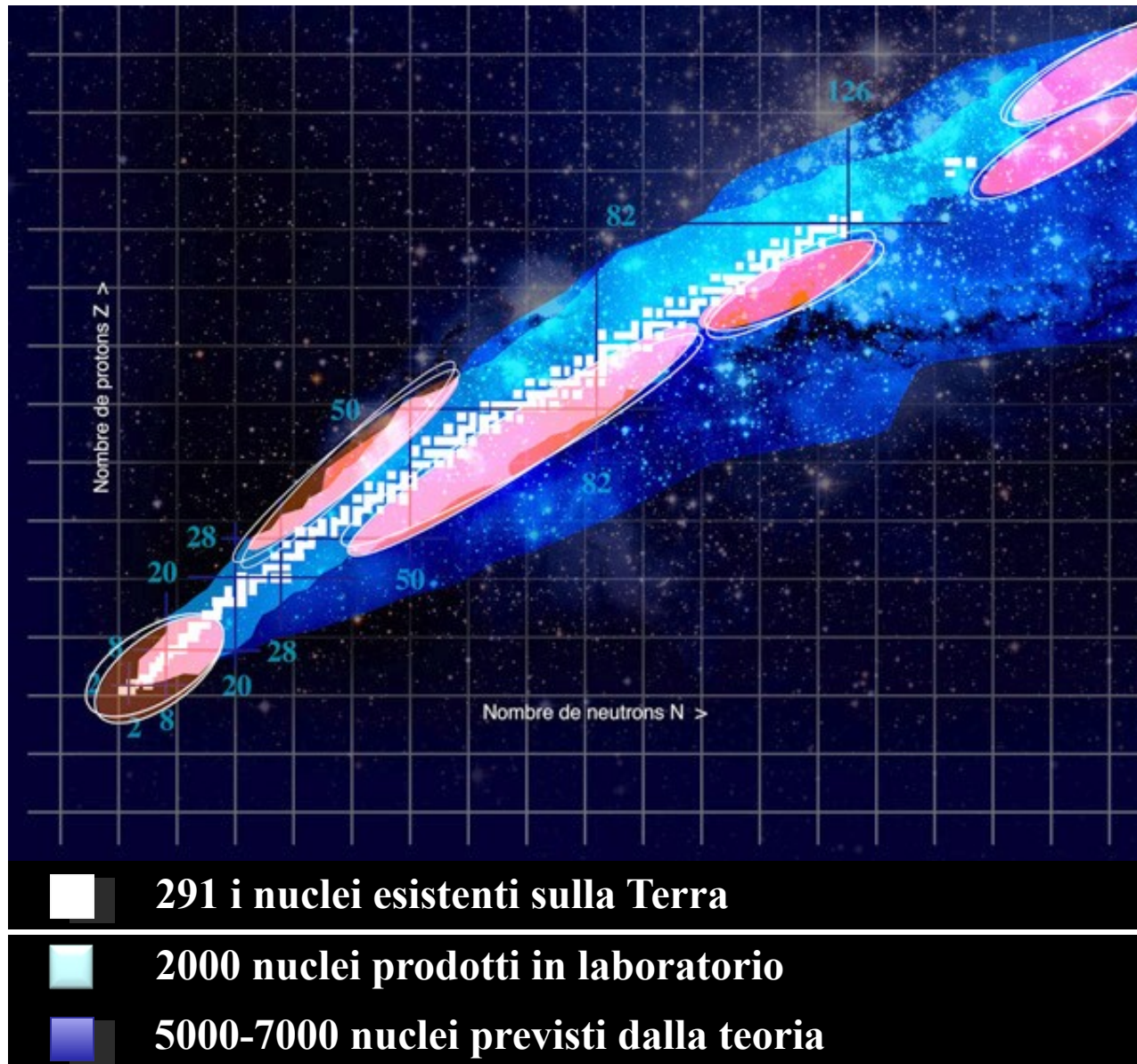


terra incognita



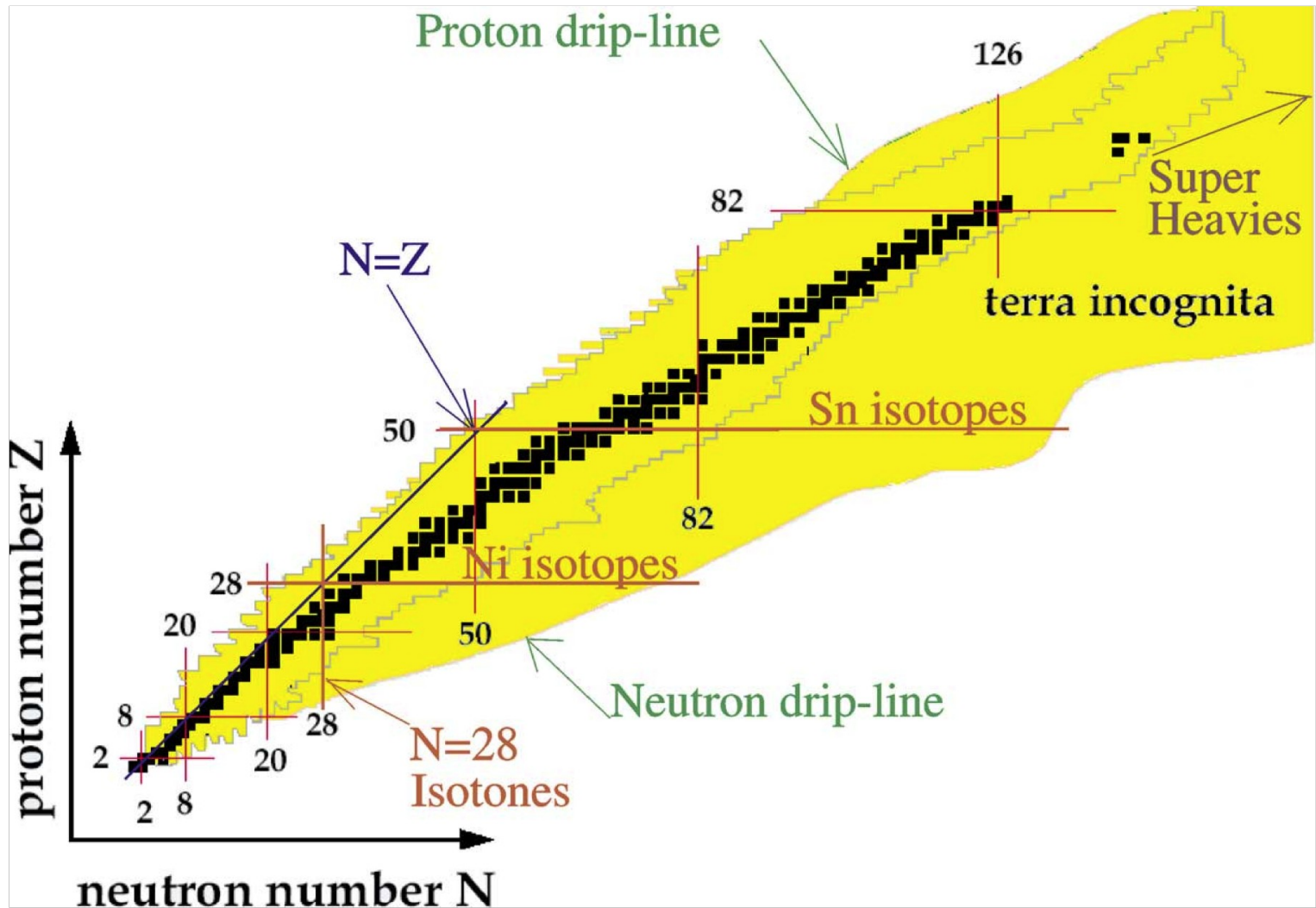


Fig. 1. Chart of nuclei showing in green the ridge of the approximately 250 stable nuclei on the island of several thousand of nuclei bound by the strong interaction but radioactive (yellow area) which constitute a real Terra Incognita since only a few percent of them have been observed up to now (thin line).

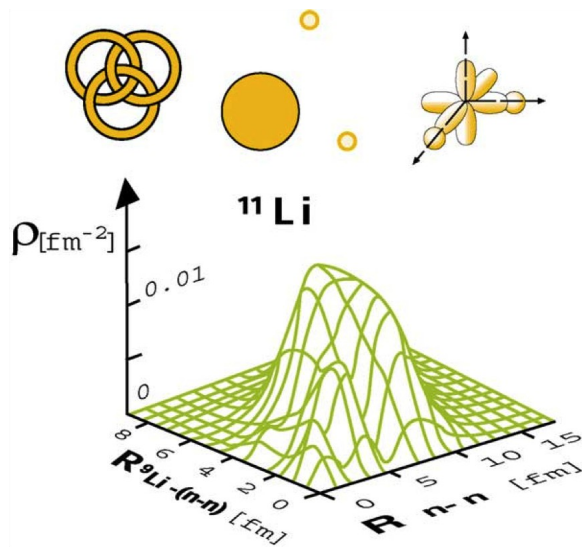


Fig. 11. Predicted probability for a certain distance between ${}^9\text{Li}$ and the neutron pair and the distance between the two neutrons. The peak corresponds to a structure, which resembles to a water molecule (see top). The drawing on the left is the symbols of the Borromee family (adapted from [42]).

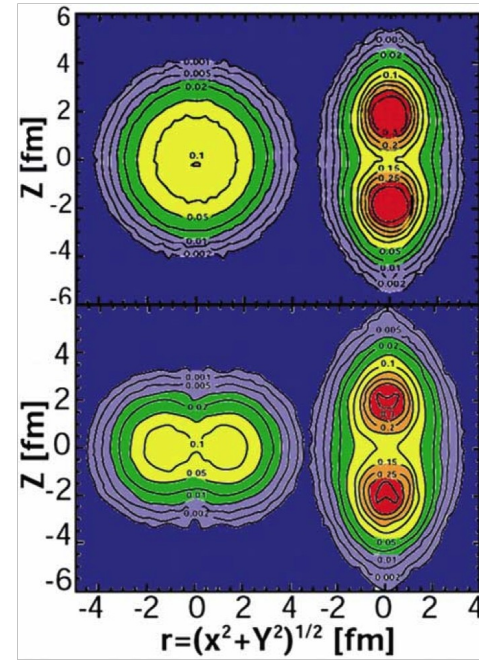


Fig. 12. Ab initio quantum calculations using Monte Carlo techniques of the density contours of ${}^8\text{Be}$ first $0+$ (top) and $4+$ (bottom). The left part is in the laboratory frame while the right part corresponds to the intrinsic frame (adapted from [45]).

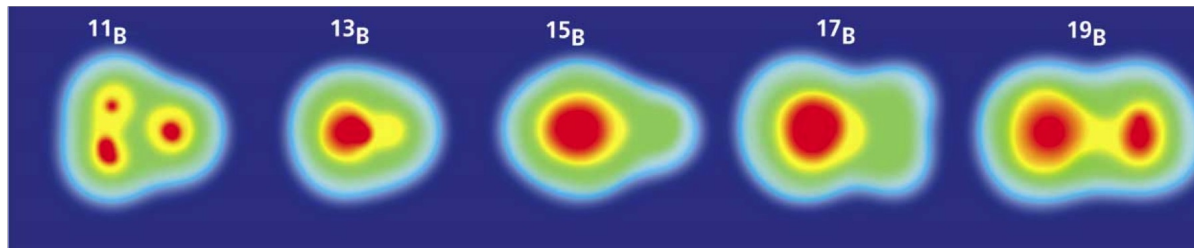


Fig. 13. Anti-symmetrized molecular dynamics calculation of the ground state of light nuclei showing a strongly clustered system (adapted from [41]).

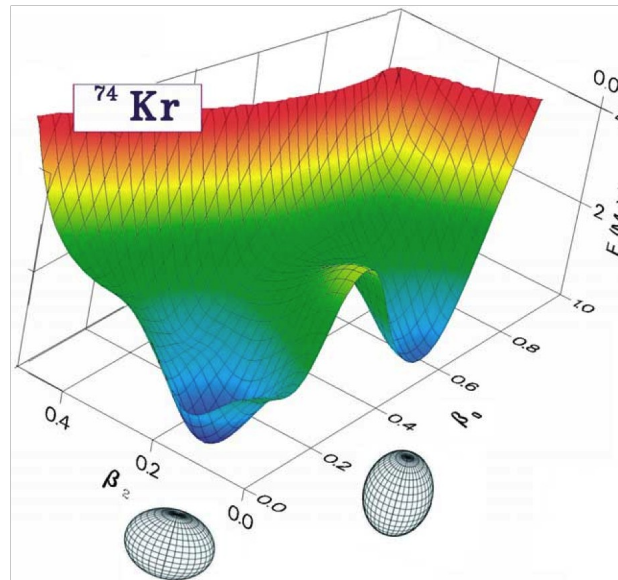


Fig. 14. Hartree–Fock–Bogoliubov calculation of the energy of a ^{74}Kr nucleus as a function of its deformation. The two deep minima correspond to two isomeric states with different shapes (shown below) (adapted from [28]).

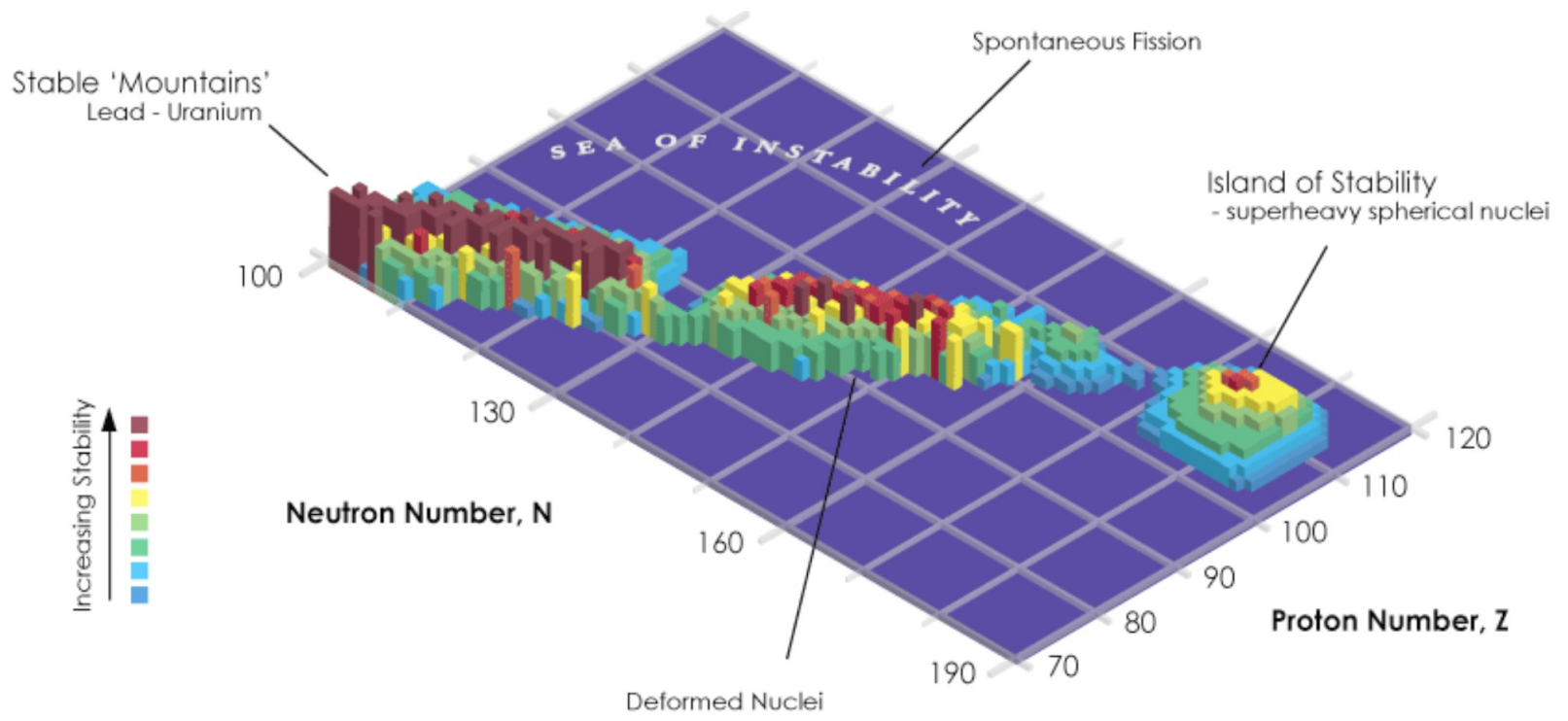
Gruppo	1	2	3	4	5	6	7	8	9	10	11	12	13	14	15	16	17	18	
Periodo																			
1	1 H																	2 He	
2	3 Li	4 Be											5 B	6 C	7 N	8 O	9 F	10 Ne	
3	11 Na	12 Mg											13 Al	14 Si	15 P	16 S	17 Cl	18 Ar	
4	19 K	20 Ca	21 Sc	22 Ti	23 V	24 Cr	25 Mn	26 Fe	27 Co	28 Ni	29 Cu	30 Zn	31 Ga	32 Ge	33 As	34 Se	35 Br	36 Kr	
5	37 Rb	38 Sr	39 Y	40 Zr	41 Nb	42 Mo	43 Tc	44 Ru	45 Rh	46 Pd	47 Ag	48 Cd	49 In	50 Sn	51 Sb	52 Te	53 I	54 Xe	
6	55 Cs	56 Ba	57 La	*	72 Hf	73 Ta	74 W	75 Re	76 Os	77 Ir	78 Pt	79 Au	80 Hg	81 Tl	82 Pb	83 Bi	84 Po	85 At	86 Rn
7	87 Fr	88 Ra	89 Ac	**	104 Rf	105 Db	106 Sg	107 Bh	108 Hs	109 Mt	110 Ds	111 Rg	112 Cn	113 Uut	114 Uuq	115 Uup	116 Uuh	117 Uus	118 Uuo

* Lantanoidi	58 Ce	59 Pr	60 Nd	61 Pm	62 Sm	63 Eu	64 Gd	65 Tb	66 Dy	67 Ho	68 Er	69 Tm	70 Yb	71 Lu
** Attinoidi	90 Th	91 Pa	92 U	93 Np	94 Pu	95 Am	96 Cm	97 Bk	98 Cf	99 Es	100 Fm	101 Md	102 No	103 Lr

Serie chimiche della tavola periodica				
Metalli alcalini	Metalli alcalino terrosi	Lantanoidi	Attinoidi	Metalli del blocco d
Metalli del blocco p	Semimetalli	Nonmetalli	Alogeni	Gas nobili

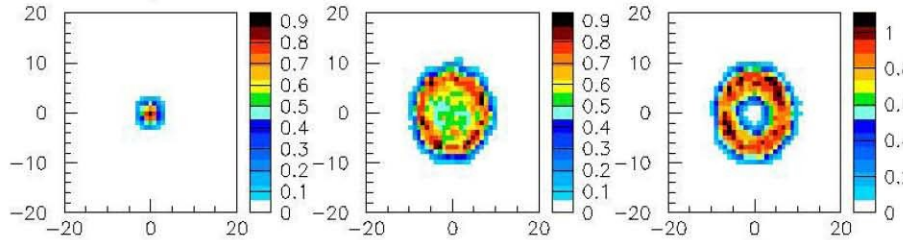
Legenda per i colori dei **numeri atomici**:

- gli elementi numerati in blu sono liquidi a $T = 298\text{ K}$ e $p = 1\text{ bar}$;
- quelli in verde sono gas a $T = 298\text{ K}$ e $p = 1\text{ bar}$;
- quelli in nero sono solidi a $T = 298\text{ K}$ e $p = 1\text{ bar}$;
- quelli in rosso sono artificiali e non sono naturalmente presenti sulla Terra (sono tutti solidi a $T = 298\text{ K}$ e $p = 1\text{ bar}$). Il [tecnecio](#) è presente in minime quantità nelle miniere di [uranio](#) e nelle [giganti rosse](#).
- quelli in grigio non sono ancora stati scoperti



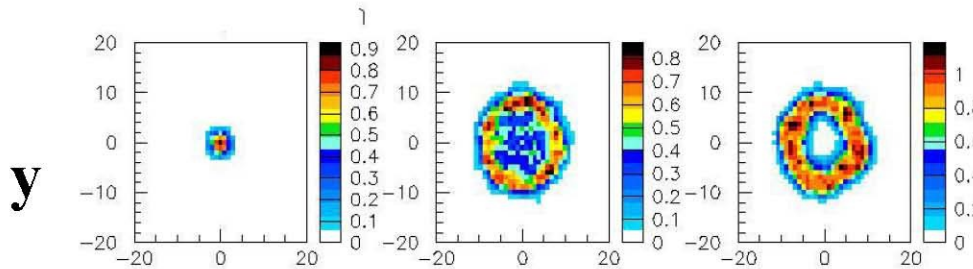
Simulation results for central collisions of Au+Au

E=15MeV/nucleon

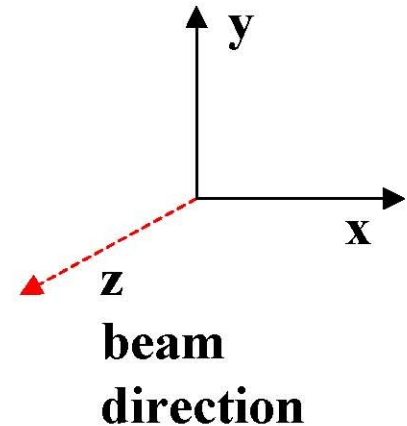
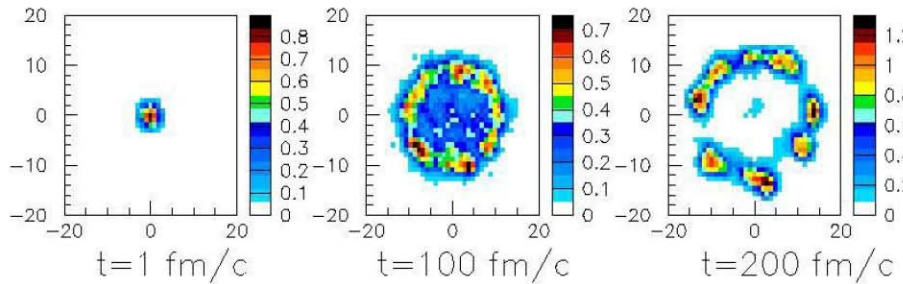


K=200MeV

E=23MeV/nucleon



E=40MeV/nucleon

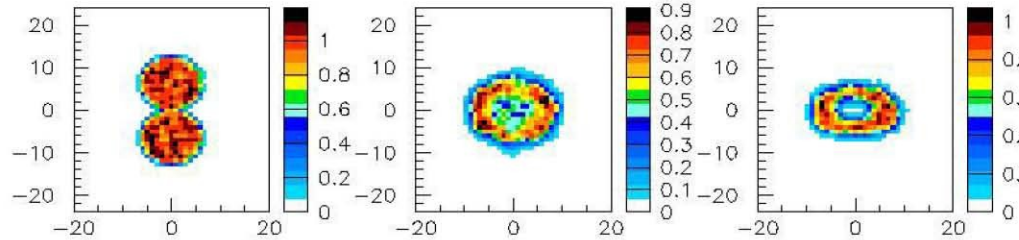


BUU calculations

X

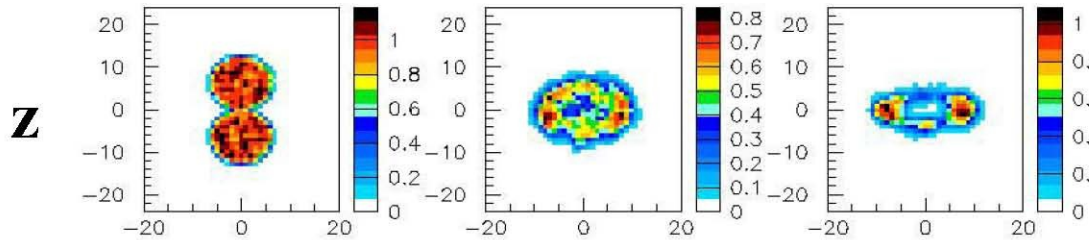
Simulation results for central collisions of Au+Au

E=15 MeV/nucleon

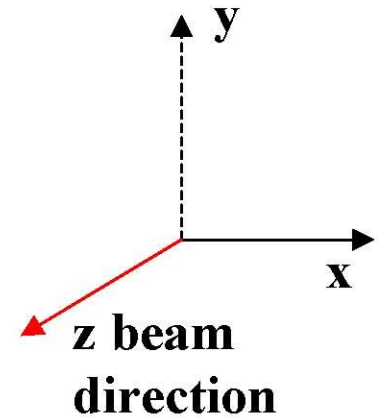
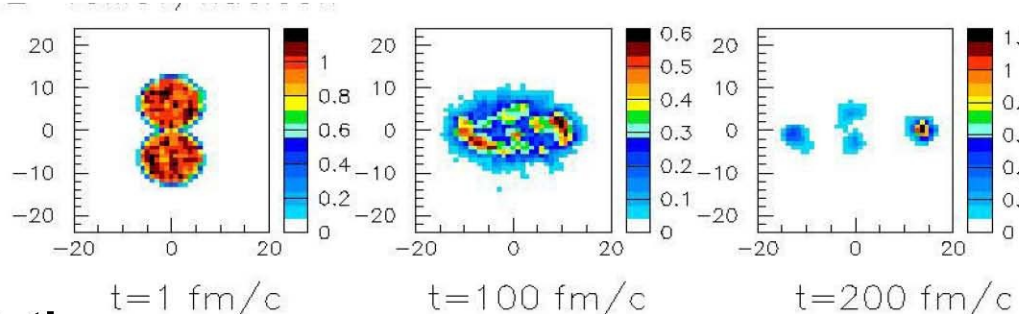


K=200 MeV

E=23 MeV/nucleon



E=40 MeV/nucleon



BUU calculations

X

Boltzmann – Uehling – Uhlenbeck model

The BUU transport equation for the nucleonic one-body density distribution function $f = f(\vec{r}, \vec{p}, t)$ is given by:

$$\left[\frac{\partial}{\partial t} + \vec{v} \nabla_r - (\nabla_r U) \nabla_p \right] f(\vec{r}, \vec{p}, t) = - \frac{1}{(2\pi)^3} \int d^3 \vec{p}_2 d^3 \vec{p}_2' d\Omega \frac{d\sigma}{d\Omega} v_{12} \left\{ f f_2 (1 - f_1')(1 - f_2') - f_1' f_2' (1 - f)(1 - f_2) (2\pi)^3 \delta^3 (\vec{p}_1 + \vec{p}_2 - \vec{p}_1' - \vec{p}_2') \right\}$$

$d\sigma/d\Omega$ - nucleon-nucleon cross section

v_{12} - relative velocity for the colliding nucleons,

U - mean-field potential consisting of the Coulomb potential and a nuclear potential with isoscalar and symmetry terms.

The potential field is approximated by

$$U(\rho, \tau_z) = A \left(\frac{\rho}{\rho_0} \right) + B \left(\frac{\rho}{\rho_0} \right)^\sigma + (1 - \tau_z) V_c + V_{n,p}^{asy}(\rho, \delta)$$

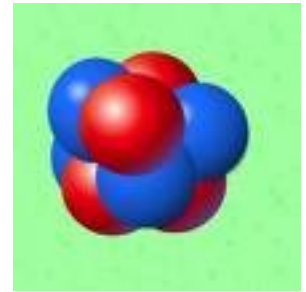
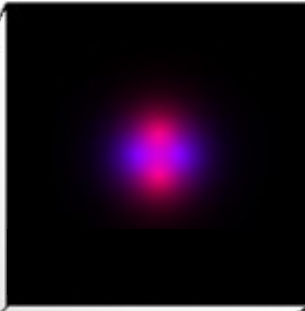
ρ_0 - normal nuclear matter density,

ρ, ρ_n, ρ_p - nucleon, neutron, and proton densities,

τ_z - equals 1 or -1 for neutrons or protons, respectively.

$\delta = (\rho_n - \rho_p) / (\rho_n + \rho_p)$ - asymmetry parameter

EOS	A[MeV]	B[MeV]	σ	K[MeV]
STIFF	-124.69	74.24	2	380
SOFT	-356	306.1	7/6	200

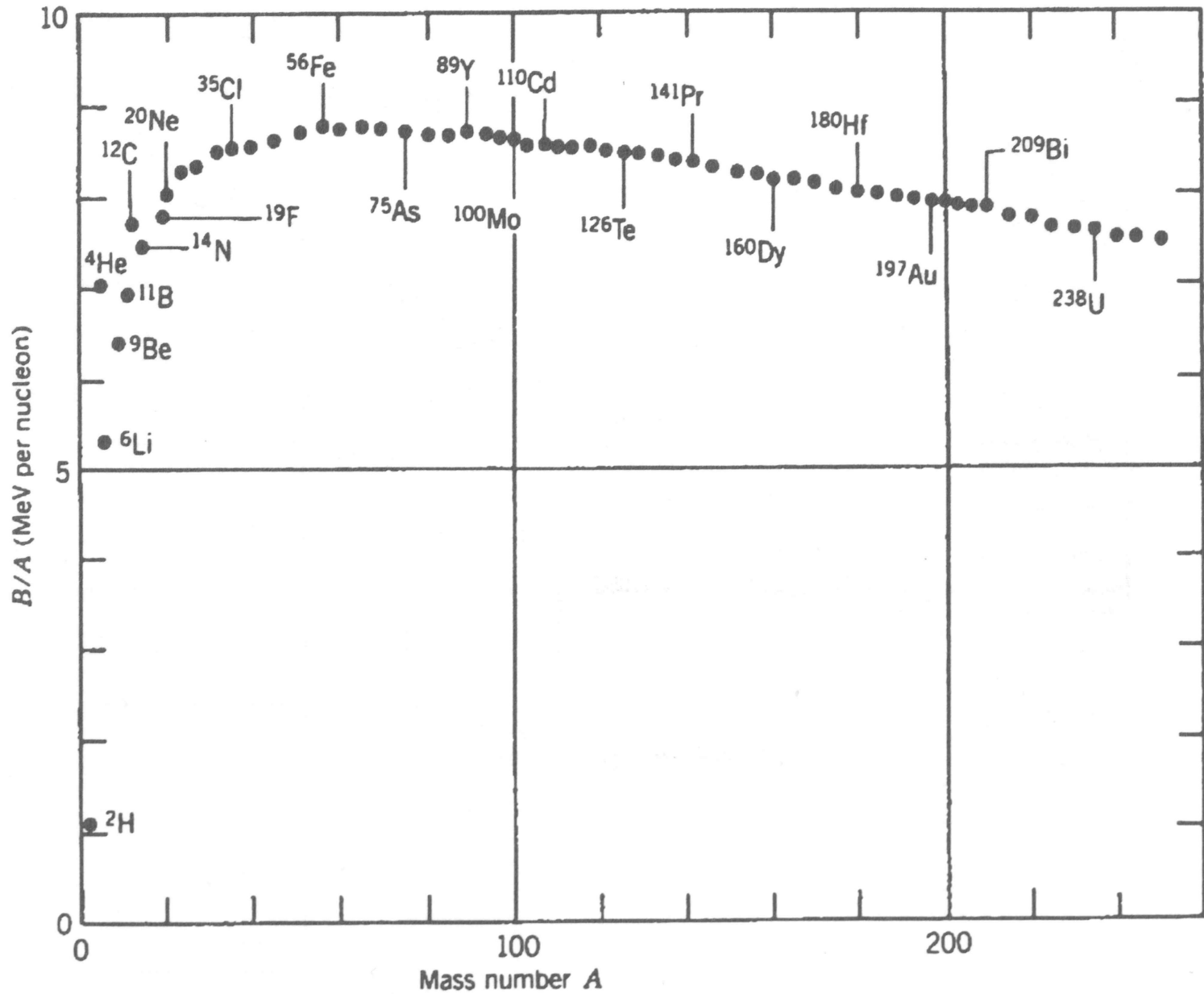


$$R_a \quad 10^{-10} \text{ m} = 0,1 \text{ nm}$$

$$R_N \quad 10^{-15} \text{ m} = 1 \text{ fm}$$

$$\text{se } R_a \quad \text{cm}$$

$$R_N \quad \text{km}$$



$$m_N \approx A(\text{amu})$$

$$V_N = \frac{4}{3} \pi r_0^3 A$$

$$n = \frac{A}{\frac{4}{3} \pi r_0^3 A} \approx 0,17 \text{ fm}^{-3}$$

$$\rho_0 = \frac{m_N}{V_N} = \frac{\text{amu}}{\frac{4}{3} \pi r_0^3} \approx$$

$$\approx \frac{1,66 \times 10^{-27}}{4,2 \times 1,5 \times 10^{-45}} \text{ kg m}^{-3} \approx$$

$$\approx 2,6 \times 10^{17} \frac{\text{kg}}{\text{m}^3} \equiv 2,6 \times 10^{14} \frac{\text{g}}{\text{cm}^3} \equiv 2,6 \times 10^8 \frac{\text{t}}{\text{cm}^3}$$

$$\frac{1}{2} m_n v^2 = kT = (1,38 \times 10^{-23}) (293) \text{ J} \approx$$

$$\approx 4 \times 10^{-21} \text{ J} \approx 25 \times 10^{-3} \text{ eV}$$

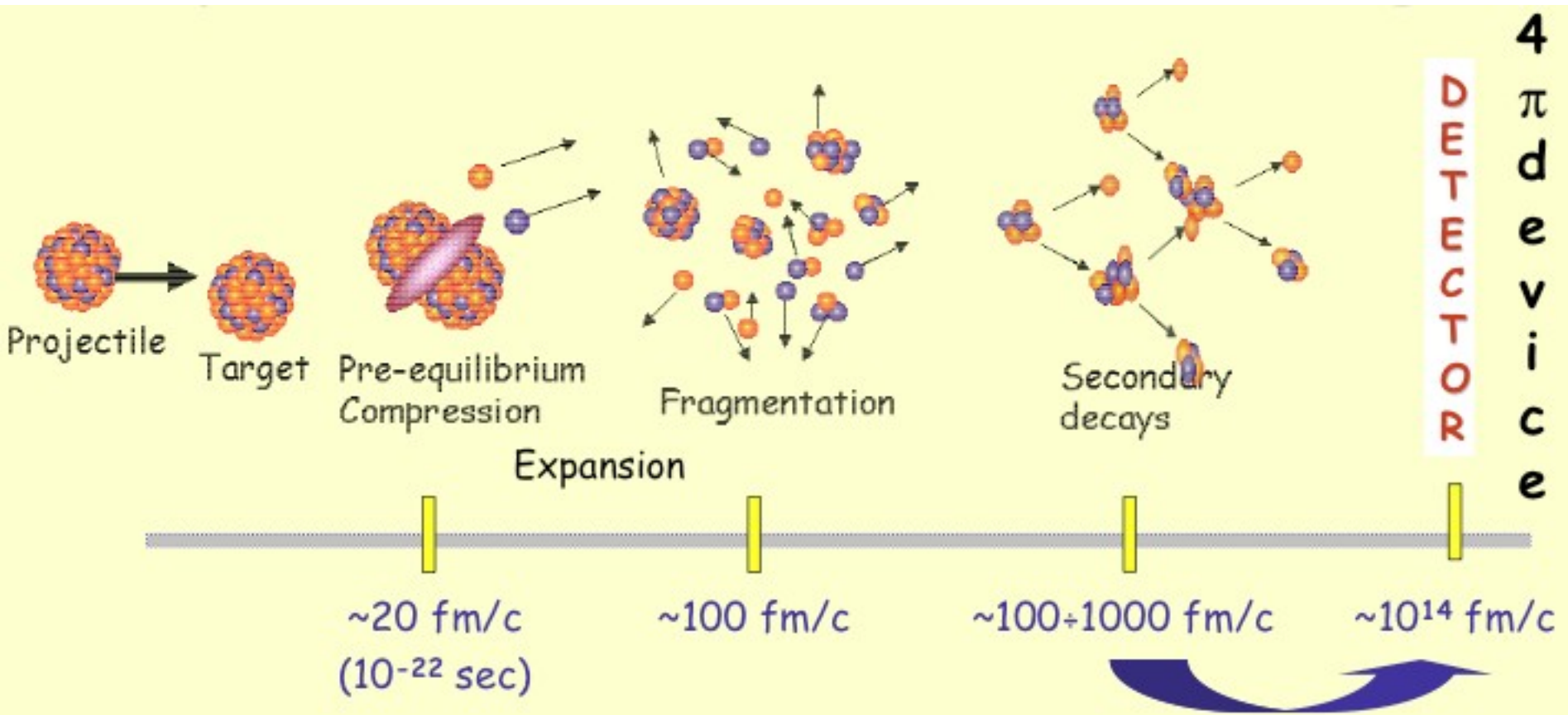
$$v = \sqrt{\frac{2kT}{m_n}} \approx \sqrt{\frac{8 \times 10^{-21}}{1,66 \times 10^{-27}}} \text{ m/s} \approx 2,2 \times 10^3 \text{ m/s}$$

$$E^* \approx 1 \text{ MeV}$$



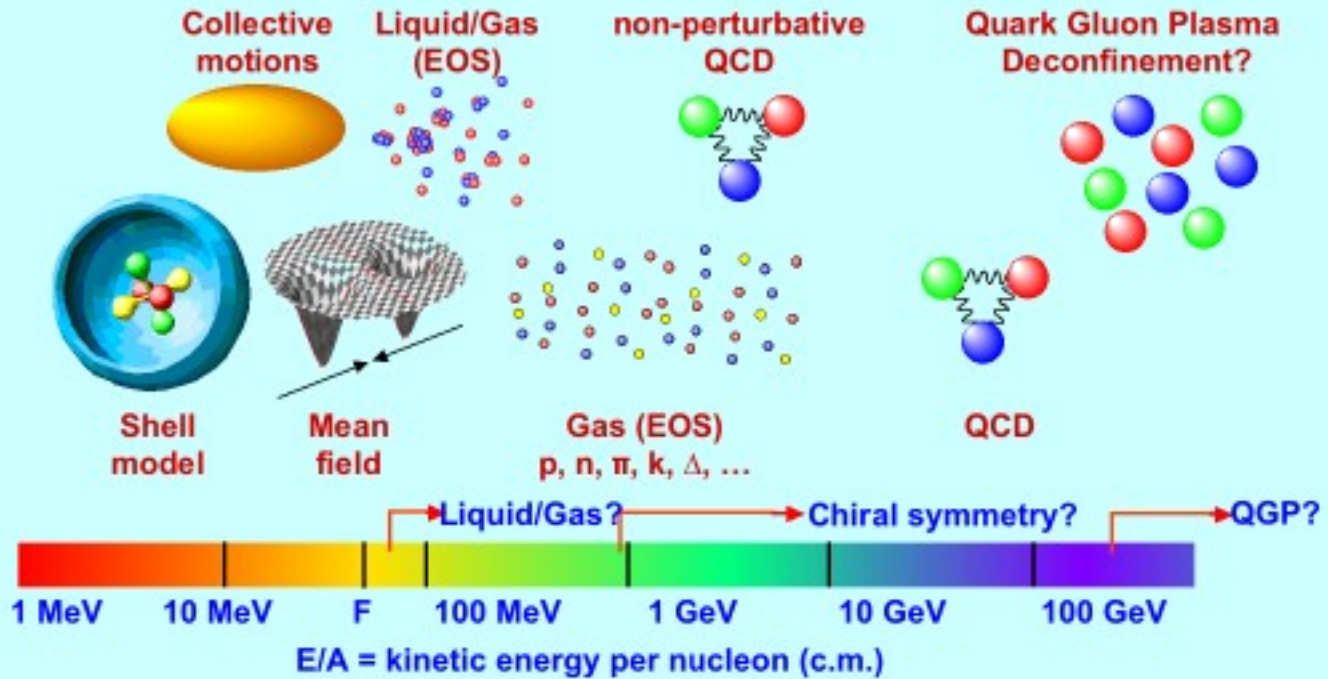
$$T \approx 11,6 \times 10^9 \text{ K}$$

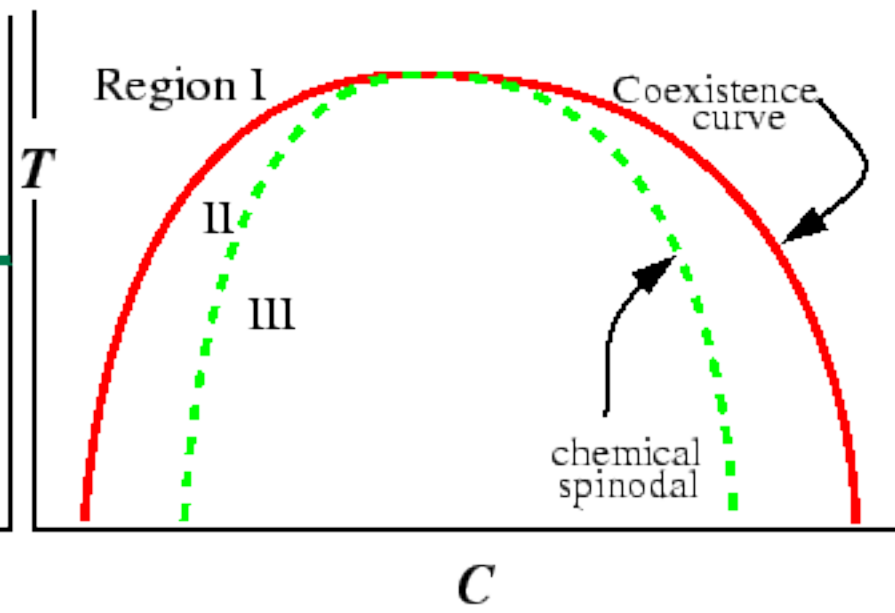
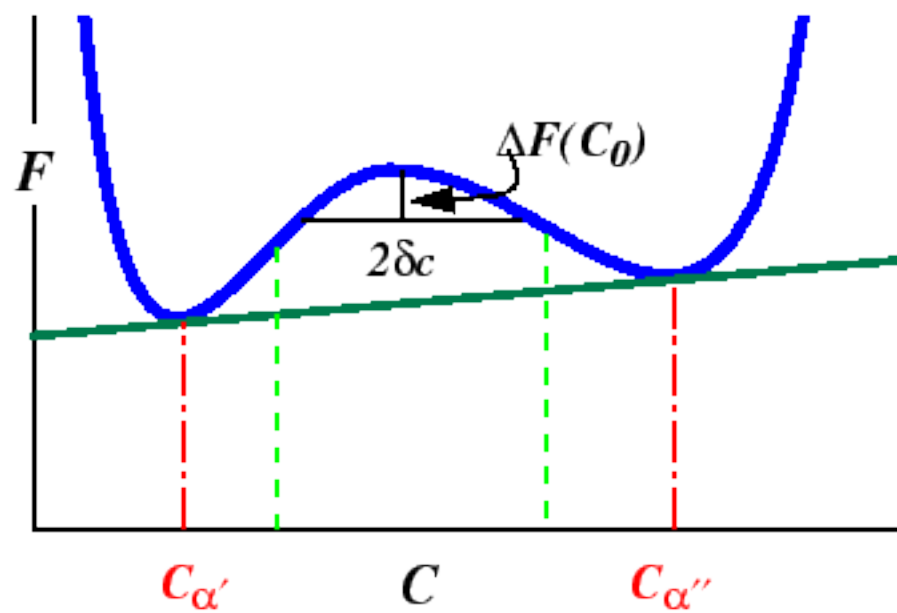
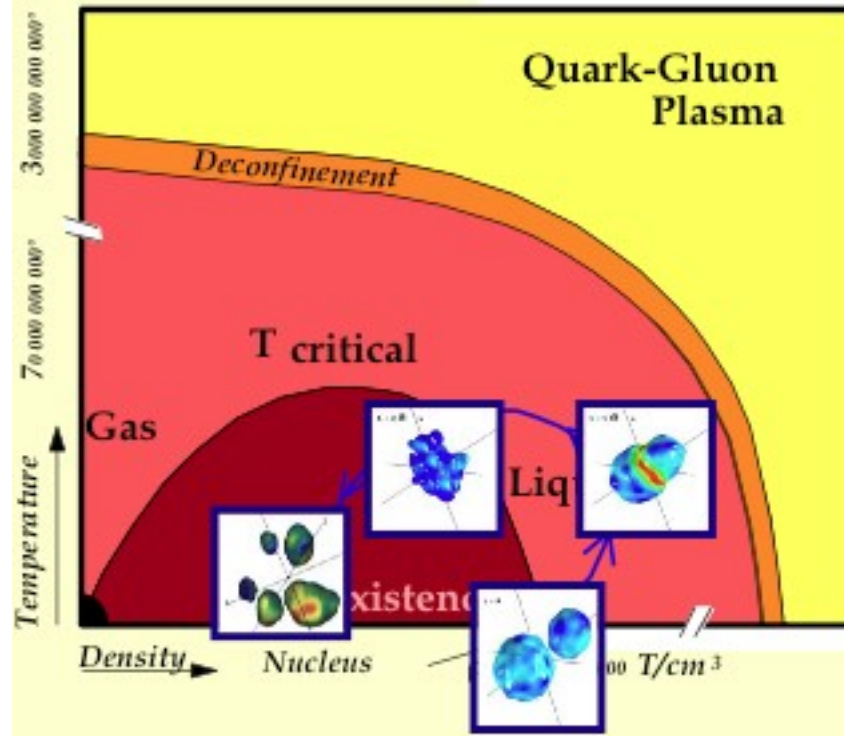
$$v \approx 1,4 \times 10^7 \text{ m/s}$$

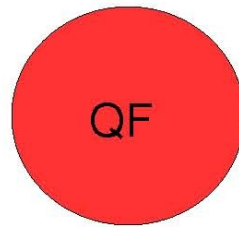
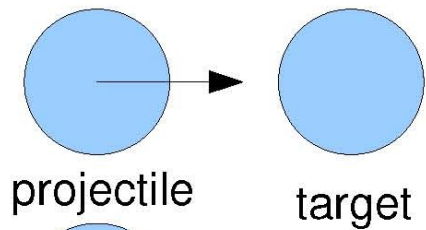


$$t_N \rightarrow \frac{fm}{c} = \frac{10^{-15}}{299\,792\,458} \approx 3,3 \times 10^{-24} \text{ s}$$

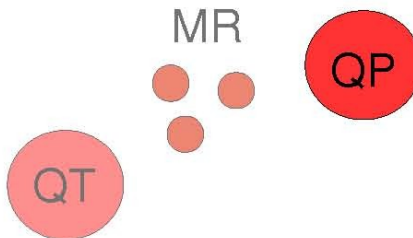
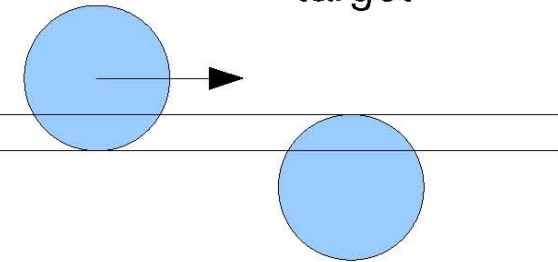
Properties of nuclear matter



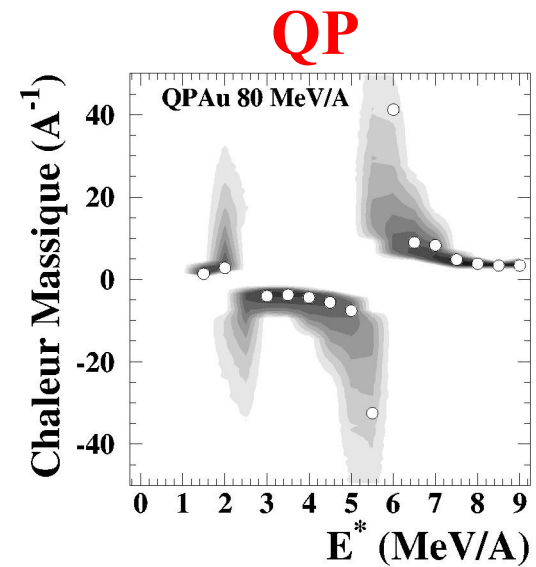
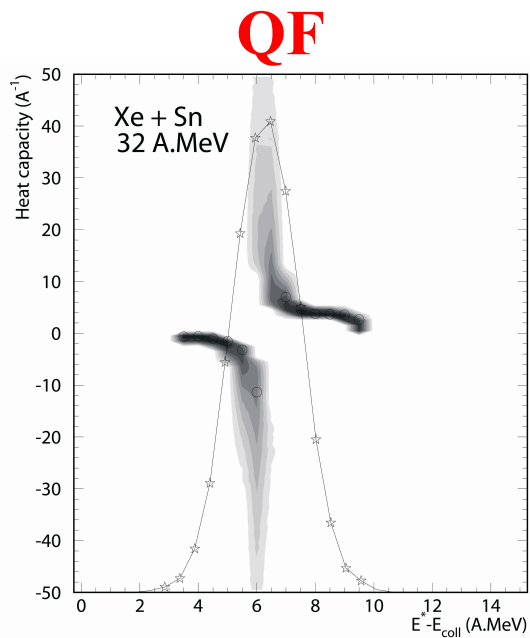




Central collisions
Quasi-Fusion (QF) sources

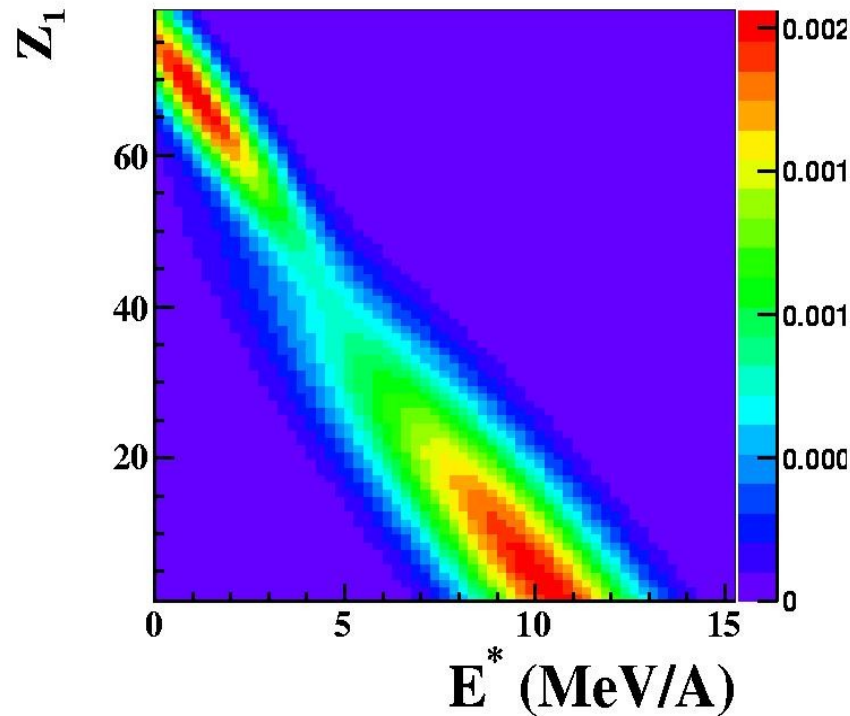


Peripheral collisions
Quasi-Projectile (QP) sources



Negative heat capacity

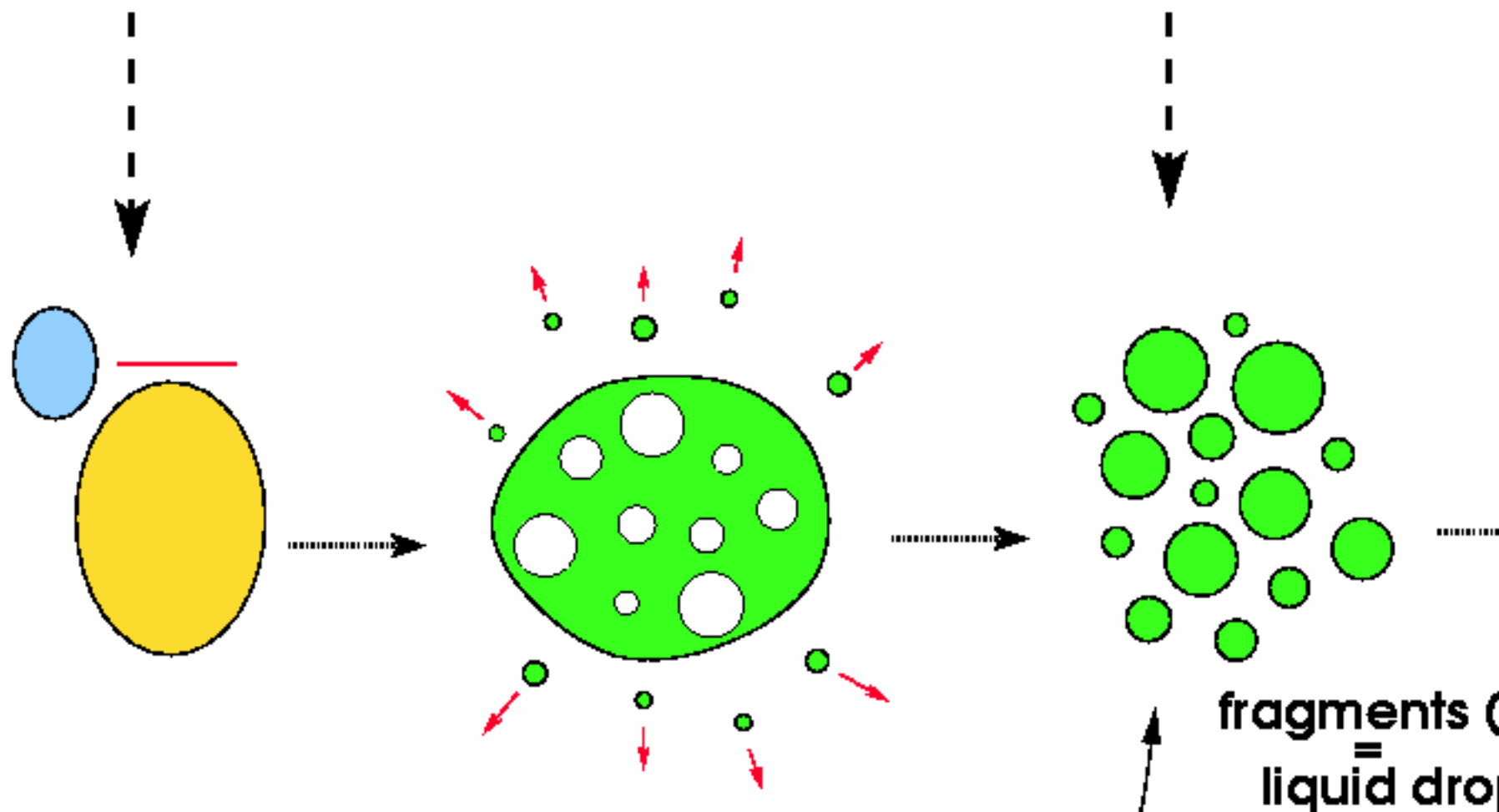
Bimodal behavior of the heaviest fragment distribution as signature of a first order phase transition in finite systems



latent heat of the phase transition for heavy nuclei $Z \sim 70$
 $(E_G - E_L) \sim 8.1 (\pm 0.4)_{\text{stat}} (\pm 1.2 - 0.9)_{\text{syst}} \text{ A MeV}$

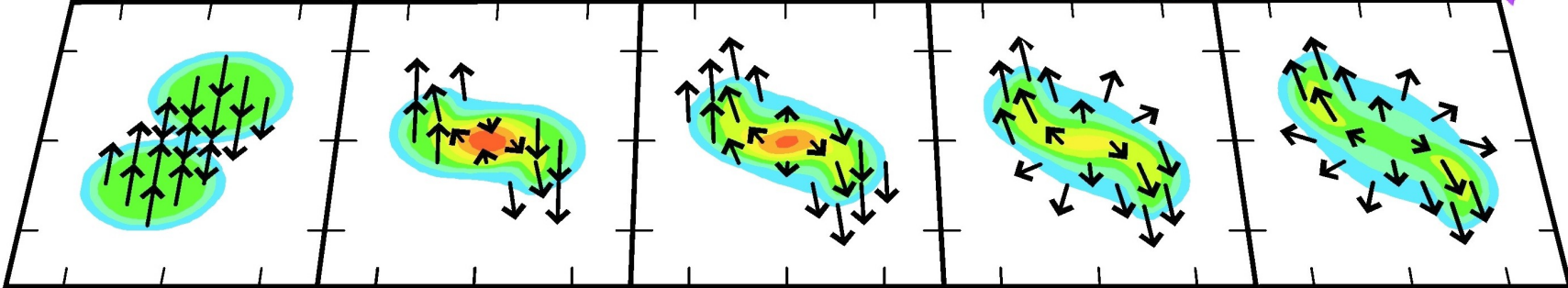
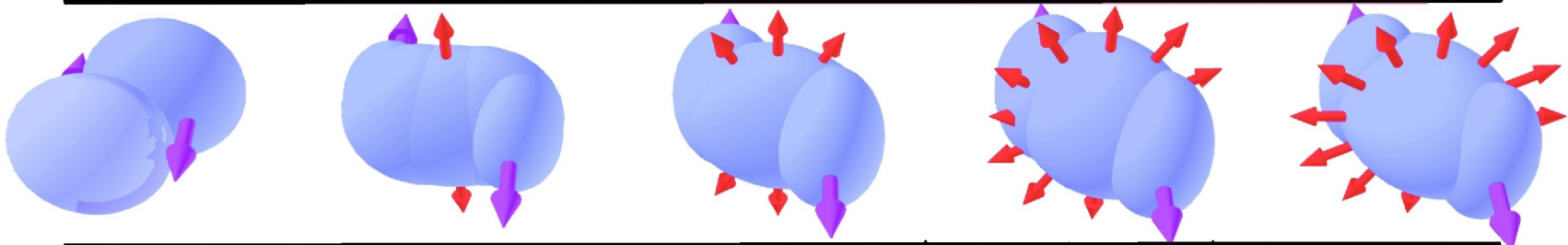
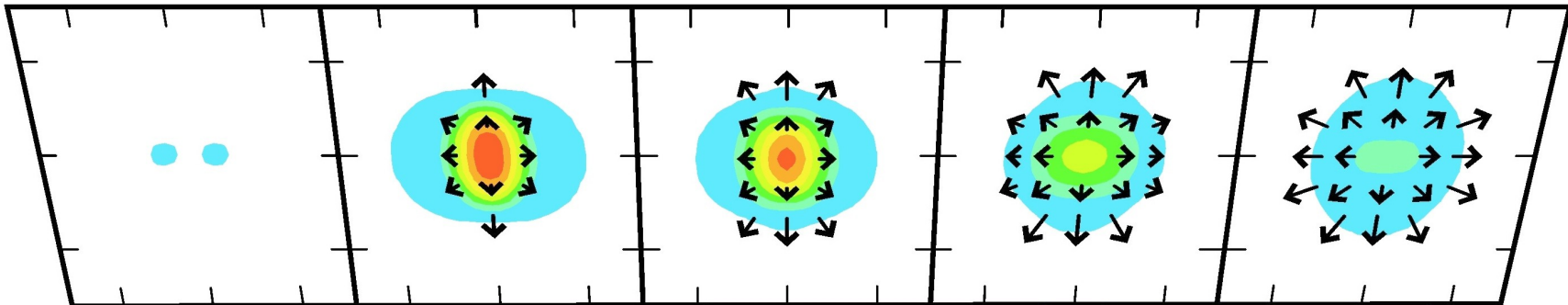
STARTING POINT
OF
DYNAMICAL MODELS

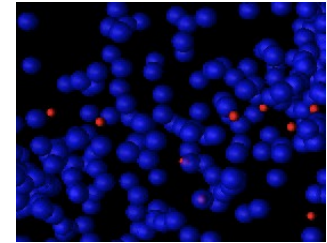
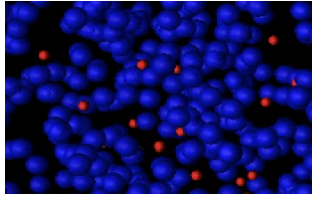
STARTING POINT
OF
STATISTICAL MODELS



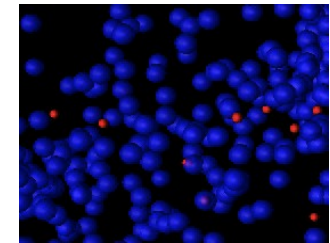
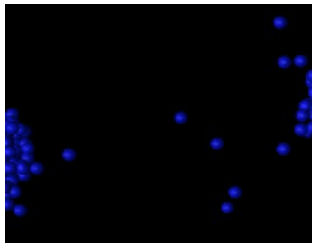
fragments (= liquid droplets)

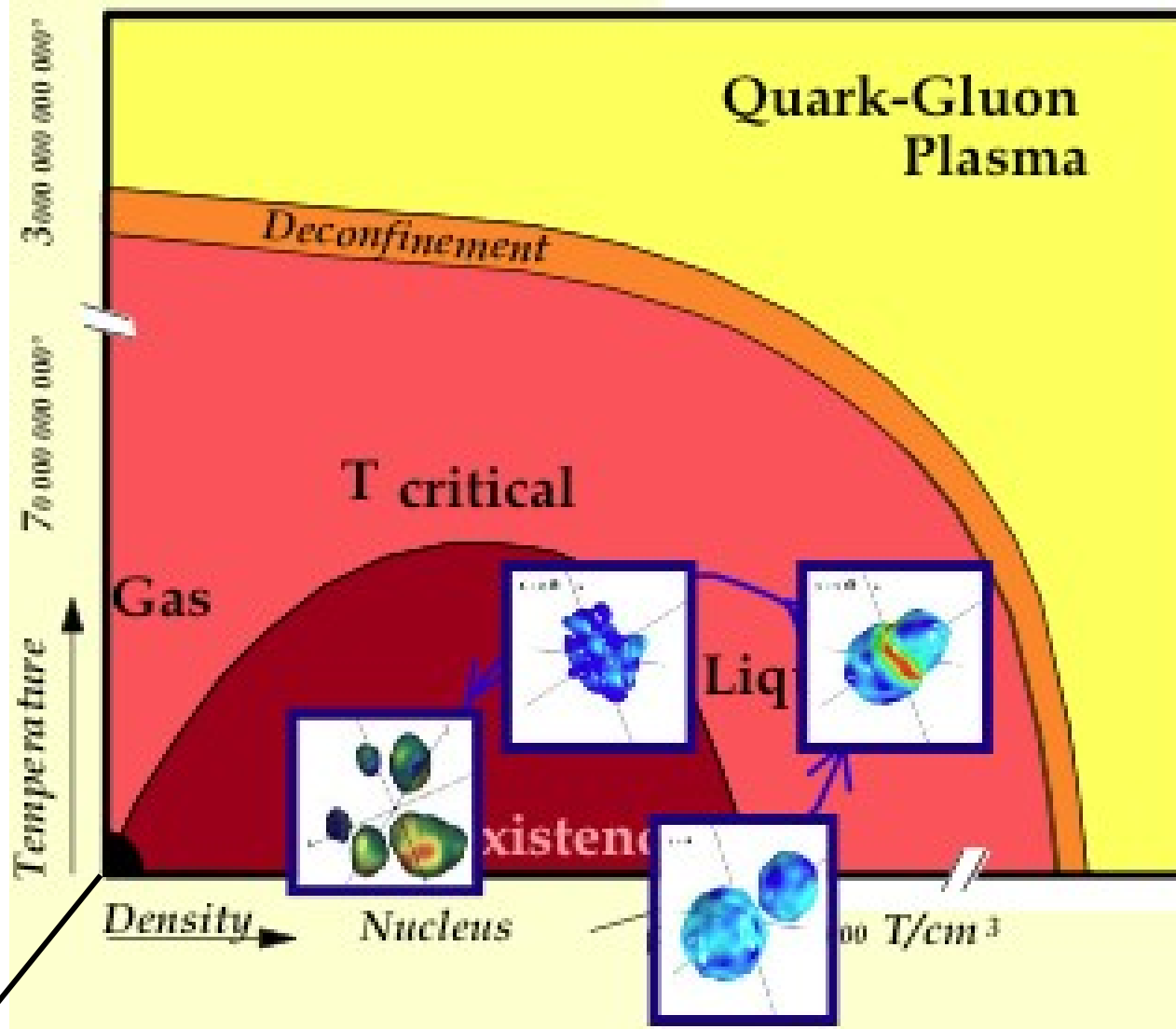
At freeze-out : thermal and chemical equilibrium





Au+Au @ $E=1A.GeV$

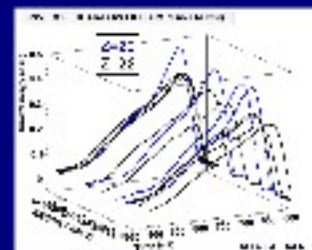




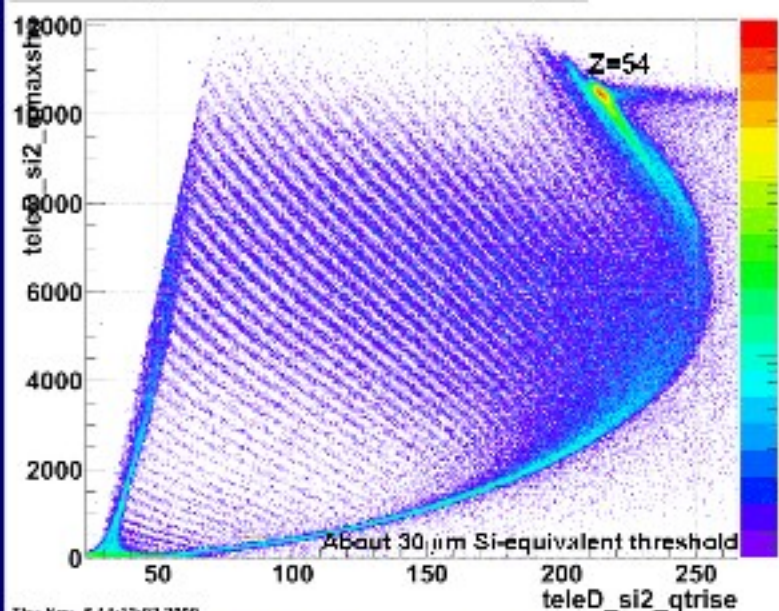
FAZIA collaboration

FAZIA PHASE-I prototype
R&D Experiment
(LNS-Nov. 2009)

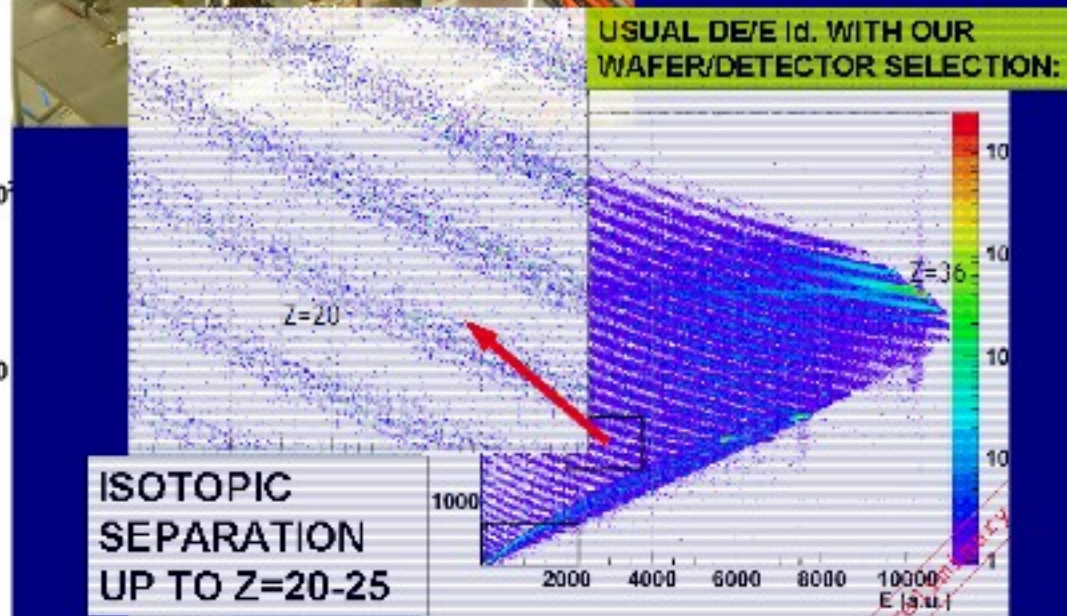
$^{129}\text{Xe} + \text{Ni}$ 35 A.MeV



ENERGY (channel) versus Q-RISE TIME (ns)



Thu Nov 5 14:12:02 2009



Z identification up to Z=54
with ONE detector by Pulse Shape Analysis

